Erb-B2 Receptor Tyrosine Kinase 2 is negatively regulated by the p53-responsive microRNA-3184-5p in cervical cancer cells

HONGLI LIU[1], YUZHI LI[1], JING ZHANG[1], NAN WU[2], FEI LIU[2], LIHUA WANG[1], YUAN ZHANG[1], JING LIU[1], XUAN ZHANG[3], SUYANG GUO[1] and HONGTAO WANG[4]

Departments of [1]Gynecological Oncology and [2]Respiration and Anhui Clinical and Preclinical Key Laboratory of Respiratory Disease, First Affiliated Hospital of Bengbu Medical College; Departments of [3]Gynecological Oncology and [4]Immunology and Anhui Key Laboratory of Infection and Immunity, Bengbu Medical College, Bengbu, Anhui 233030, P.R. China

Received November 30, 2019; Accepted October 2, 2020

DOI: 10.3892/or.2020.7862

Abstract. The oncogenic role of Erb-B2 Receptor Tyrosine Kinase 2 (ERBB2) has been identified in several types of cancer, but less is known on its function and mechanism of action in cervical cancer cells. The present study employed a multipronged approach to investigate the role of ERBB2 in cervical cancer. ERBB2 and microRNA (miR)-3184-5p expression was assessed in patient-derived cervical cancer biopsy tissues, revealing that higher levels of ERBB2 and lower levels of miR-3184-5p were associated with clinicopathological indicators of cervical cancer progression. Furthermore, ERBB2 stimulated proliferation, migration and sphere-formation of cervical cancer cells *in vitro*. This effect was mediated by enhanced phosphatidylinositol-4,5-bisphosphate 3-kinase catalytic subunit α activity. Additionally, it was revealed that miR-3184-5p directly suppressed ERBB2 in cervical cancer cells. The p53 activator Mithramycin A stimulated p53 and miR-3184-5p expression, thereby lowering the levels of ERBB2 and attenuating proliferation, migration and sphere-formation of cervical cancer cells. In conclusion, the findings of the present study suggested ERBB2 as an oncogenic protein that may promote invasiveness in cervical cancer cells. Treatment of cervical cancer cells with the p53 activator Mithramycin A restored the levels of the endogenous ERBB2 inhibitor miR-3184-5p and may represent a novel treatment strategy for cervical cancer.

Correspondence to: Mr. Hongtao Wang, Department of Immunology and Anhui Key Laboratory of Infection and Immunity, Bengbu Medical College, 2600 Donghai Road, Bengbu, Anhui 233030, P.R. China
E-mail: bb_wanghongtao@126.com

Key words: cervical cancer, Erb-B2 Receptor Tyrosine Kinase 2, microRNA-3184-5p, p53

Introduction

Among women, cervical cancer is ranked 4th in global cancer-associated deaths (1), with over half a million deaths in 2012 (2). Cervical cancer can be broadly categorized into squamous cell carcinoma, which constitutes the majority of cases (70-80%) or adenocarcinoma, which comprises 10-15% of cases (3). Cervical cancer is frequently caused by the oncovirus human papillomavirus (HPV), mainly by types HPV-16 and -18 in ~70% of patients with cervical cancer (3). The molecular drivers of the formation and development of cervical cancer are often due to recurrent mutations within the PI3K/AKT signaling pathway (4-7) or from deactivating, loss-of-function mutations in the tumor suppressor TP53 gene (p53 protein), which produces a particularly aggressive phenotype (8). Additionally, altered expression levels of microRNAs (miRNAs/miRs), which are short, regulatory, non-coding RNAs, have been implicated in metastatic cervical cancer (9,10). Among miRNAs associated with cervical cancer (11-13), miR-3184 has been identified as a p53-responsive miRNA (14). However, its mechanistic role in cervical oncogenesis remains unknown.

Erb-B2 Receptor Tyrosine Kinase 2 (ERBB2), also known as human epidermal growth factor receptor 2, is an established oncogenic protein associated with tumorigenesis, cancer progression and acquisition of therapy resistance in breast, esophagogastric and colorectal cancer (15-17). However, the involvement of ERBB2 in cervical cancer development is less well known (18). Mithramycin A is an antibacterial and anticancer agent that was first purified from *Streptomyces* bacteria (19-21). It binds to G/C-rich stretches of DNA within minor grooves (19), which is one of its possible mechanisms for its antitumor properties (22). Mithramycin A possesses a favorable safety profile and inhibits tumor proliferation *in vivo* in cervical cancer murine xenograft models (23). Another possible mechanism for the antitumor effects of Mithramycin A is via p53 activation (24); however, in cervical cancer, the influence of Mithramycin A on p53 and ERBB2 has not been examined.

Phosphatidylinositol-4,5-bisphosphate 3-kinase catalytic subunit α (PIK3CA) is the catalytic subunit of PI3K (25). In humans, PIK3CA acts as a proto-oncogene that supports

proliferation and metastasis of tumor cells (25), and PIK3CA copy number gains are associated with higher-grade tumors and poor patient prognosis in several malignancies, including gastric, thyroid and prostate cancer (25). In patients with cervical cancer, *PIK3CA* mutations are significantly associated with shorter survival times (*PIK3CA* mutant median survival of 67.1 months vs. non-mutant median survival of 90.3 months) (26). The aforementioned evidence suggests that targeting PIK3CA activity may be a rational approach in combating cervical cancer. Therefore, the present study aimed to examine the association between the effects of the p53-responsive miR-3184-5p, ERBB2 and PIK3CA in cervical cancer.

Materials and methods

Patient samples. The present study was approved by the Ethics Review Committee of the First Affiliated Hospital of Bengbu Medical College (approval no. 201858; Bengbu, China). Patients who donated cervical cancer tissues gave their informed consent in writing prior to their involvement in the study. All specimens were harvested following biopsy or surgery (cone biopsy, radical trachelectomy or radical hysterectomy) at the aforementioned hospital between March 2000 and March 2002 from female patients (median age, 53 years; age range, 35-65 years) that had never received chemo- or radiotherapy, yielding 65 pairs of primary cervical cancer samples and matched healthy cervical tissue samples (>2 cm from the tumor edge). Tumor specimens were staged by a licensed pathologist according to the International Federation of Gynecologists and Obstetricians (FIGO) staging system (27). The specimens were immediately kept in liquid nitrogen and frozen at -80˚C until further use.

Cell lines, culture conditions and general materials. Human cervical cancer HeLa and SiHa cell lines were obtained from the American Type Culture Collection. The non-cancerous, HPV-immortalized H8 cell line of cervical epithelial squamous cells was obtained from The Cell Bank of Type Culture Collection of the Chinese Academy of Sciences. Cells were grown in DMEM/F12 with 10% FBS (both from Invitrogen; Thermo Fisher Scientific, Inc.) at 37˚C in a 5% CO_2 incubator. Reverse transcription-quantitative PCR (RT-qPCR) was regularly employed to check for contaminating mycoplasma (*MycoITSF9* forward primer, 5'-ACA CCA TGG GAG CTG GTA AT-3' and reverse primer, 5'-CTT CAT CGA CTT TCA GAC CCA AGG CA-3'), as previously described (28). Mithramycin A and general lab reagents were purchased from Sigma-Aldrich (Merck KGaA). For *in vitro* experiments, Mithramycin A dissolved in DMSO at concentrations of 0 (vehicle control), 50 and 100 nM was used to treat cells for 48 h at 37˚C in a 5% CO_2 incubator.

Transfections. SiHa cells were transfected with plasmid vectors, while HeLa cells were transfected with small-interfering RNAs (siRNAs). pCMV6-XL4/5 plasmid vectors containing the TrueClone® human cDNA sequences for human *TP53* (NM_000546; cat. no. SC119832), *PIK3CA* (NM_006218; cat. no. SC116227) or *ERBB2* (NM_004448; cat. no. SC128161), and an empty negative control (NC) plasmid vector (cat. no. PCMV6XL5) were obtained from OriGene Technologies, Inc. For plasmid transfections, cells were seeded in 6-well plates ($1.5x10^5$ cells/well) and transiently transfected with 1 μg plasmid using Lipofectamine® 3000 transfection reagent (Invitrogen; Thermo Fisher Scientific, Inc.) for 20 min at room temperature and then incubated in fresh medium at 37˚C for an additional 48 h prior to subsequent experimentation. siRNAs targeting human *ERBB2* (ERBB2-siRNA; cat. no. sc-29405), human *PIK3CA* (PIK3CA-siRNA; cat. no. sc-39127) and scrambled control (scr-siRNA; cat. no. sc-37007) were obtained from Santa Cruz Biotechnology, Inc. For siRNA transfections, cells were seeded in 6-well plates ($2x10^5$ cells/well) and transiently transfected with 80 pmol siRNA using Lipofectamine 3000 transfection reagent for 7 h at 37˚C and then incubated in fresh medium at 37˚C for an additional 48 h prior to subsequent experimentation. miR-3184-5p (miRBase accession no. MIMAT0015064) mirVana® miRNA mimic (cat. no. 4464066) and mirVana® miRNA inhibitor (cat. no. 4464084), as well as the corresponding controls (cat. nos. 4464058 and 4464078, respectively), were obtained from AmbionÒ (Thermo Fisher Scientific, Inc.). For miRNA mimic/inhibitor transfections, HeLa and SiHa cells were seeded in 6-well plates ($1x10^5$ cells/well) and transiently transfected with 3 nM mimic or 10 nM inhibitor using Lipofectamine 3000 transfection reagent for 48 h at 37˚C prior to subsequent experimentation.

RT-qPCR. TRIzol® (Invitrogen; Thermo Fisher Scientific, Inc.) was used to extract total RNA from cells or tissue samples, of which a 100-ng aliquot from every sample was used for cDNA preparation using the PrimeScript™ RT Reagent Kit according to the manufacturer's protocol (Takara Bio, Inc.). A SuperScript™ III Platinum™ SYBR™ Green One-Step qRT-PCR kit or NCode™ SYBR™ Green miRNA qRT-PCR kit (both from Invitrogen; Thermo Fisher Scientific, Inc.) was used to quantify mRNA or miR-3184-5p expression, respectively, on an ABI PRISM™ 7000 Sequence Detection System (Applied Biosystems; Thermo Fisher Scientific, Inc.). The mRNA qPCR thermocycling conditions were as follows: 95˚C for 3 min, followed by 45 cycles of 95˚C for 15 sec and 60˚C for 45 sec. The miRNA qPCR thermocycling conditions were as follows: 50˚C for 2 min and 95˚C for 2 min, followed by 40 cycles of 95˚C for 15 sec and 60˚C for 50 sec. The following primers were obtained from OriGene Technologies, Inc., and Applied Biosystems (Thermo Fisher Scientific, Inc.): ERBB2 forward, 5'-GGA AGT ACA CGA TGC GGA GACT-3' and reverse, 5'-ACC TTC CTC AGC TCC GTC TCTT-3'; CD44 forward, 5'-CCA GAA GGA ACA GTG GTT TGGC-3' and reverse, 5'-ACT GTC CTC TGG GCT TGG TGTT-3'; CD133 forward, 5'-CAC TAC CAA GGA CAA GGC GTTC-3' and reverse, 5'-CAA CGC CTC TTT GGT CTC CTTG-3'; Aldehyde Dehydrogenase 1 (ALDH1) forward, 5'-CGG GAA AAG CAA TCT GAA GAG GG-3' and reverse, 5'-GAT GCG GCT ATA CAA CAC TGGC-3'; SNAIL forward, 5'-TGC CCT CAA GAT GCA CAT CCGA-3' and reverse, 5'-GGG ACA GGA GAA GGG CTT CTC-3'; vimentin forward, 5'-AGG CAA AGC AGG AGT CCA CTGA-3' and reverse, 5'-ATC TGG CGT TCC AGG GAC TCAT-3'; E-cadherin forward, 5'-GCC TCC TGA AAA GAG AGT GGA AG-3' and reverse, 5'-TGG CAG TGT CTC TCC AAA TCCG-3'; PIK3CA

forward, 5'-GAA GCA CCT GAA TAG GCA AGT CG-3' and reverse, 5'-GAG CAT CCA TGA AAT CTG GTC GC-3'; GAPDH forward, 5'-GCG AGA TCC CTC CAA AAT CAA-3' and reverse, 5'-GTT CAC ACC CAT GAC GAA CAT-3'; and small nuclear RNA (snRNA) U6 forward, 5'-CTC GCT TCG GCA GCA CAT-3' and reverse, 5'-TTT GCG TGT CAT CCT TGCG-3'. The forward primer for miR-3185-5p possessed the same sequence as the mature miR-3184-5p strand, while the reverse primer for miR-3185-5p was the universal reverse primer supplied with the NCode™ SYBR™ Green miRNA qRT-PCR Kit (Invitrogen; Thermo Fisher Scientific, Inc.). GAPDH and snRNA U6 served as internal standardization controls for mRNAs and miRNAs, respectively. Relative expression levels were calculated using the $2^{-\Delta\Delta Cq}$ method (29).

Western blotting (WB). Cells or tissue samples were lysed using M-PER™ Mammalian Protein Extraction Reagent (Pierce; Thermo Fisher Scientific, Inc.) and protein content was quantified using a Bio-Rad Protein Assay kit (Bio-Rad Laboratories, Inc.). Proteins (30 μg/lane) were separated via 12% SDS-PAGE and transferred to polyvinylidene difluoride (PVDF) membranes. The membranes were rinsed, blocked with 5% skimmed milk in TBST (20 mM Tris, 150 mM NaCl, 0.05% Tween-20) for 2 h at room temperature, and incubated at 4˚C overnight with the following primary antibodies (all diluted 1:1,000 unless otherwise specified): ALDH1 (cat. no. ab9883; Abcam), total AKT1 (1:2,000; cat. no. ab28422; Abcam), phosphorylated (p-)AKT1 (S473; 1:5,000; cat. no. ab81283; Abcam), CD44 (1:2,000; cat. no. ab157107; Abcam), CD133 (cat. no. ab19898; Abcam), E-cadherin (1:50; cat. no. ab1416; Abcam), ERBB2 (cat. no. ab16901; Abcam), GAPDH (cat. no. sc-25778; Santa Cruz Biotechnology, Inc.), total mTOR (1:2,000; cat. no. ab2732; Abcam), p-mTOR (S2448; cat. no. ab109268; Abcam), p21 (mouse monoclonal; F-5; cat. no. sc-6246; Santa Cruz Biotechnology, Inc.), p53 (mouse monoclonal; DO-1; cat. no. sc-126; Santa Cruz Biotechnology, Inc.), PIK3CA (cat. no. ab40776; Abcam), SNAIL (cat. no. ab53519; Abcam) and vimentin (cat. no. ab92547; Abcam). Membranes were then rinsed and incubated for 1 h at room temperature with species-appropriate, HRP-conjugated secondary antibodies (1:5,000; cat. nos. ab7090 and ab97110; Abcam), rinsed and analyzed using an ECL Western Blotting Detection kit (Amersham; Cytiva). ImageJ version 1.46 software (National Institutes of Health) was used for blot densitometry analysis.

Evaluation of invasion by Transwell assay. BioCoat™ Matrigel® Invasion Chambers (Corning, Inc.) were used to evaluate the invasive capacity of cervical cancer cell lines according to previous studies (30,31). Cervical cancer cells ($5x10^4$) that had undergone transfection were plated into the top chamber in serum-free medium, while complete medium (with 10% FBS) was added to the lower chambers. The Invasion Chamber was incubated for 1 day at 37˚C in a 5% CO_2 incubator, after which a cotton swab was used to remove cells from the top chamber. The remaining cells that had invaded through the Transwell membrane were fixed with ice-cold 100% methanol for 5 min and stained with 0.05% Giemsa for 30 min at room temperature. The cell numbers were counted and recorded using a light microscope at x400 magnification.

Quantification of cell viability. A Cell Counting Kit-8 (CCK-8; Dojindo Molecular Technologies, Inc.) was employed to quantify cell viability. A total of $1x10^4$ cervical cancer cells/well seeded in 96-well culture plates were incubated for 72 h at 37˚C, after which CCK-8 reagent (10 μl/well) was added for a further 4 h at 37˚C. A microplate reader measured the colorimetric signal at 450 nm.

Assessment of sphere formation. Dissociated cells were plated in 6-well Ultra-Low Attachment plates (Corning, Inc.) at a density of 5,000 cells/ml in serum-free DMEM/F12 supplemented with N-2 supplement (Invitrogen; Thermo Fisher Scientific, Inc.), epidermal growth factor (20 ng/ml), basic fibroblast growth factor (20 ng/ml) and heparin (4 mg/ml). A serum-free medium containing additional growth factors is the standard medium used for sphere formation experiments (32-34). Every well was replenished with new media every 3 days for 2 weeks at room temperature, after which spheroids with diameters >50 μm were counted manually using an inverted phase contrast light microscopy at x100 magnification.

Immunoprecipitation (IP). For the initial IP step, 10 μg anti-ERBB3 antibody or IgG control antibody (cat. nos. 4754 and 2729, respectively; Cell Signaling Technology, Inc.) was incubated with protein G magnetic beads according to the manufacturer's protocol (Pierce; Thermo Fisher Scientific, Inc.) in 150 mM NaCl/100 mM HEPES (pH 8.2) buffer for 2 h at 4˚C to form the anti-ERBB3-protein G beads or anti-IgG-protein G beads, respectively. After washing, 300 μg cell lysate protein (obtained using M-PER™ Mammalian Protein Extraction Reagent; Pierce; Thermo Fisher Scientific, Inc.) was immunoprecipitated on a rotator overnight at 4˚C using 20 μl antibody-protein G beads. The antibody-protein G beads were then collected by pulse centrifugation (5 sec at 14,000 x g) at 4˚C. The antibody-protein G beads were washed with lysis buffer, SDS-sample buffer with dithiothreitol (50 mM) was added, and the samples were boiled for 4 min. The samples were electrophoresed on a 4-12% bis-tris gel followed by transfer to a PVDF membrane. Co-IP with ERBB2 or PI3K (p85) was assessed via WB, as aforementioned, using an anti-ERBB2 antibody or anti-PI3K (p85) antibody (1:1,000; cat. no. ab16901 and ab191606, respectively; Abcam).

TargetScan analysis and luciferase reporter assay. The TargetScan database (www.targetscan.org) was used to search for candidate miRNAs that may bind to the ERBB2 3'-untranslated region (UTR). A pMirTarget firefly luciferase reporter plasmid (cat. no. PS100062) containing the wild-type (WT) 3'-UTR of human ERBB2 (ERBB2-3'-UTR^{WT}; cat. no. SC208188) was obtained from OriGene Technologies, Inc. Mutations were introduced using a QuikChange™ Site-Directed Mutagenesis kit (Agilent Technologies, Inc.) into the putative miR-3184-5p binding site on ERBB2-3'-UTR^{WT} to create the mutant (MU) ERBB2-3'-UTR^{MU}. Subsequently, transfection of cervical cancer cells using Lipofectamine 3000 transfection reagent was performed using the following: One of the firefly luciferase reporter plasmids (ERBB2-3'-UTR^{WT} or ERBB2-3'-UTR^{MU}), a transfection standardization pGL4.74[hRluc/TK] *Renilla* reporter plasmid (cat. no. E692;

Promega Corporation) and one of the miRNAs (miR-3184-5p mimic or inhibitor, or their corresponding negative controls). After 1 day of transfection, bioluminescence from luciferase activity was analyzed using a Dual-Luciferase Reporter Assay System (cat. no. E1910; Promega Corporation). Relative luciferase intensity was obtained as the intensity of the firefly to *Renilla* luciferase signal for each experimental condition, which was then expressed relative to the respective control conditions, whose values were taken as 1.0.

Statistical analysis. All data are expressed as the mean ± SEM, unless otherwise specified. Data were analyzed using SPSS 24.0 (IBM Corp.). Comparisons of expression levels in cervical cancer tissues vs. matched healthy cervical tissues were assessed using a Wilcoxon signed-rank test, while comparisons between independent tumor tissue samples were assessed using a Mann-Whitney U test. Kaplan-Meier survival analyses were stratified based on median expression levels, with high levels being above the median and low levels being below the median; comparisons between survival curves were analyzed using a log-rank test. For *in vitro* experiments, an unpaired two-tailed Student's t-test or one-way ANOVA with Bonferroni post-hoc testing was employed for comparisons between 2 or ≥3 groups, respectively. $P<0.05$ was considered to indicate a statistically significant difference.

Results

ERBB2 expression is upregulated in cervical cancer tissues and is associated with a poor prognosis. The clinicopathological characteristics of the 65 recruited patients with cervical cancer are presented in Table SI. ERBB2 mRNA and protein expression was significantly higher in cervical cancer tissues compared with in matched healthy cervical tissues (Fig. 1A and B). Furthermore, tumor ERBB2 transcript and protein expression was significantly upregulated in advanced FIGO stages compared with in early FIGO stages (Fig. 1C and D), as well as in lymph node metastatic disease compared with in non-metastatic disease (Fig. 1E and F). Subsequently, the prognostic significance of ERBB2 expression on the survival of patients with cervical cancer was evaluated. The median ERBB2 transcript expression was used to divide patients with cervical cancer into the high (above the median) or low (below the median) ERBB2 expression groups. High ERBB2 mRNA expression was associated with a poorer survival outcome compared with low ERBB2 expression (Fig. 1G). Overall, the data demonstrated that ERBB2 expression was positively associated with clinicopathological indicators of cervical cancer progression.

Upregulated ERBB2 expression in cervical cancer cell lines promotes viability, invasion and sphere formation. After discovering the association between increased ERBB2 expression and cervical cancer progression, the present study investigated the effects of ERBB2 in cervical cancer cells. The SiHa and HeLa cell lines were used as the cervical cancer cell lines, while the non-cancerous cervical epithelial H8 cell line was used as the negative control. In agreement with patient-derived samples, ERBB2 mRNA and protein expression was significantly higher in HeLa and SiHa cells compared with in H8 cells (Fig. S1). The SiHa cell line, which expressed comparatively less endogenous ERBB2 than the HeLa cell line, underwent transient transfection with an ERBB2 overexpression (OE) vector (ERBB2 vec) and an empty control plasmid (Ctrl vec). On the other hand, the HeLa cell line, which expressed comparatively high endogenous ERBB2 compared with the SiHa cell line, underwent transient transfection with an ERBB2-targeting siRNA to knock down (KD) its expression (siERBB2) or a control scrambled siRNA (siCtrl). OE or KD of ERBB2 protein was validated via WB (Fig. 2A).

Invasion was assessed via Transwell assay. siERBB2 cells invaded significantly less than siCtrl cells (Fig. 2B), while ERBB2 vec cells invaded significantly more than Ctrl vec cells (Fig. 2C), implying that upregulated ERBB2 expression stimulated the invasion of cervical cancer cells *in vitro*. Cell viability was measured using the CCK-8 assay. Cell viability in siERBB2 cells was significantly lower than that in siCtrl cells, while cell viability in ERBB2 vec cells was significantly higher than that in Ctrl vec cells (Fig. 2D). Cancer stem cell (CSC)-like characterization was evaluated via sphere formation assays. siERBB2 cells had a significantly lower sphere-forming capacity than siCtrl cells (Fig. 2E), while ERBB2 vec cells had a significantly higher sphere-forming capacity than Ctrl vec cells (Fig. 2F). The results suggested that ERBB2 promoted the viability and stemness of cervical cancer cell lines.

Since ERBB2 stimulated an invasive and CSC-like phenotype in cervical cancer cells, the transcript and protein expression levels of three metastasis-associated genes (SNAIL, E-cadherin and vimentin) and three CSC biomarkers (CD44, CD133 and ALDH1) (35,36) were measured following ERBB2 KD or OE. The results revealed that siERBB2 cells expressed lower expression levels of CD44, CD133, ALDH1, SNAIL and vimentin, but higher expression levels of E-cadherin compared with siCtrl cells (Fig. 2G). Conversely, ERBB2 vec cells expressed higher expression levels of CD44, CD133, ALDH1, SNAIL and vimentin, but lower expression levels of E-cadherin compared with Ctrl vec cells (Fig. 2G). Overall, the current results supported a role for ERBB2 in cervical cancer cell viability, invasion and stemness.

ERBB2 promotes cervical cancer cell viability and invasion by stimulating PIK3CA activity. PI3K is an oncogenic protein complex that supports the proliferation and metastasis of tumor cells (25). PI3K is formed by an active catalytic subunit (p110, also known as PIK3CA) associating with a p85 regulatory subunit, which regulates the activity of PIK3CA (37). The ERBB2-ERBB3 complex is known to bind to p85, thereby promoting PIK3CA activity and AKT phosphorylation (Fig. 3A) (38-40). Thus, IP was used to validate if the ERBB2-ERBB3 complex associated with p85 in cervical cancer cells. ERBB2 and p85 were enriched in the anti-ERBB3 IP fraction compared with in the anti-IgG control IP fraction; these effects were diminished by ERBB2-KD and potentiated by ERBB2-OE (Fig. 3B). PIK3CA transcript and protein expression was analyzed via RT-qPCR and WB, respectively. siERBB2 cells expressed similar levels of PIK3CA transcript and protein to siCtrl cells, as well as ERBB2 vec cells to Ctrl vec cells (Fig. 3C-F). To validate these findings, an OE vector was used to overexpress PIK3CA (PIK3CA vec) in HeLa

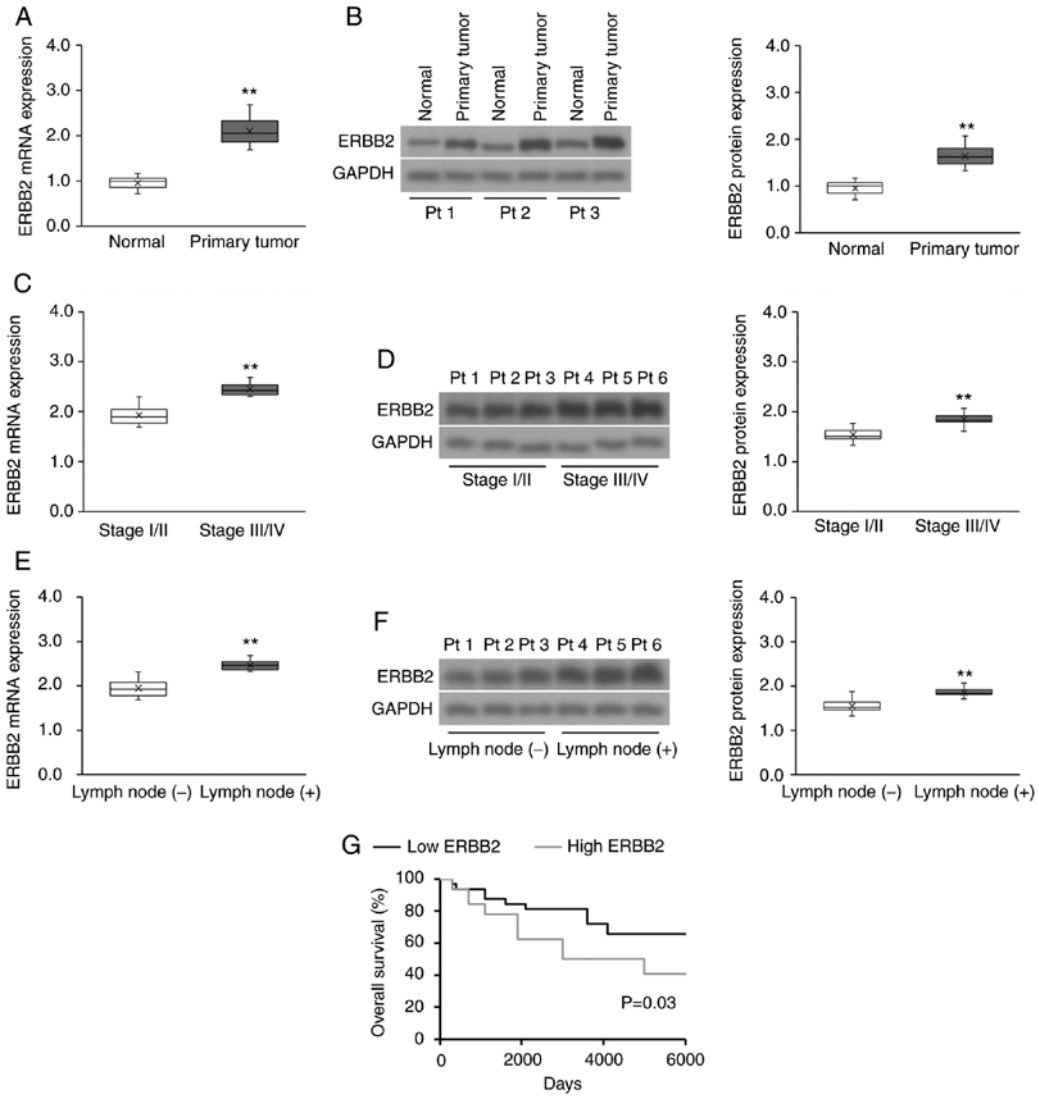

Figure 1. ERBB2 expression is upregulated in patient-derived cervical cancer tissues and is associated with a poor prognosis. (A) RT-qPCR and (B) WB analysis of ERBB2 transcript and protein expression, respectively, in patient-derived cervical cancer tissues (n=65) vs. matched healthy cervical tissues (n=65). Data were analyzed via Wilcoxon signed-rank test. (C) RT-qPCR and (D) WB analysis of ERBB2 transcript and protein expression, respectively, in stage I/II vs. stage III/IV patient-derived cervical cancer tissues (n=43 stage I/II; n=22 Stage III/IV). Data were analyzed via Mann-Whitney U test. (E) RT-qPCR and (F) WB analysis of ERBB2 transcript and protein expression, respectively, in lymph node metastatic and non-metastatic patient-derived cervical cancer biopsies [n=46 lymph node (-); n=19 lymph node (+)]. Data were analyzed via Mann-Whitney U test. (G) Survival analysis using the Kaplan-Meier method according to high (above the median) or low (below the median) ERBB2 mRNA expression (n=32 in each cohort). The P-value was calculated using the log-rank test. For purposes of comparison across cohorts, the median ERBB2 mRNA and protein expression levels (normalized to the RT-qPCR housekeeping control and WB loading control GAPDH) in the normal cohort have been set to 1.0. Data in box plots are expressed as the median ± IQRs (boxes) and absolute ranges (whiskers). n=3. **P<0.01. RT-qPCR, reverse transcription-quantitative PCR; WB, western blotting; ERBB2, Erb-B2 Receptor Tyrosine Kinase 2; Pt, patient.

cells and a PIK3CA-targeting siRNA (siPIK3CA) was used to silence PIK3CA in SiHa cells (Fig. S2A and B). Additional co-transfection of siERBB2 cells with PIK3CA vec significantly upregulated PIK3CA transcript and protein expression in HeLa cells, while additional co-transfection of ERBB2 vec cells with siPIK3CA significantly downregulated PIK3CA transcript and protein expression in SiHa cells (Fig. 3C-F).

As AKT is directly phosphorylated by PIK3CA (41) and mTOR is a known downstream target of the ERBB2-PIK3CA-AKT axis (42), the expression levels of AKT phosphorylation (p-AKT/AKT) and mTOR phosphorylation (p-mTOR/mTOR) were assessed as indicators of PIK3CA activity. siERBB2 cells expressed significantly lower AKT and mTOR phosphorylation levels compared with siCtrl cells, while ERBB2 vec cells expressed significantly higher AKT and mTOR phosphorylation levels compared with Ctrl vec cells (Fig. 3E and F). The addition of PIK3CA vec partially rescued siERBB2-induced downregulation of AKT and mTOR phosphorylation levels, while the addition of siPIK3CA partially abrogated ERBB2 vec-induced upregulation of AKT and mTOR phosphorylation levels (Fig. 3E and F). Since modulating ERBB2 expression significantly affected ERBB3-PI3K(p85) binding and downstream AKT/mTOR phosphorylation, but did not change PIK3CA expression, the present results indicated that ERBB2 promoted PIK3CA activity via regulating the ERBB3-PI3K(p85) interaction.

Subsequently, the current study examined if PIK3CA participated in ERBB2-facilitated stimulation of HeLa cell

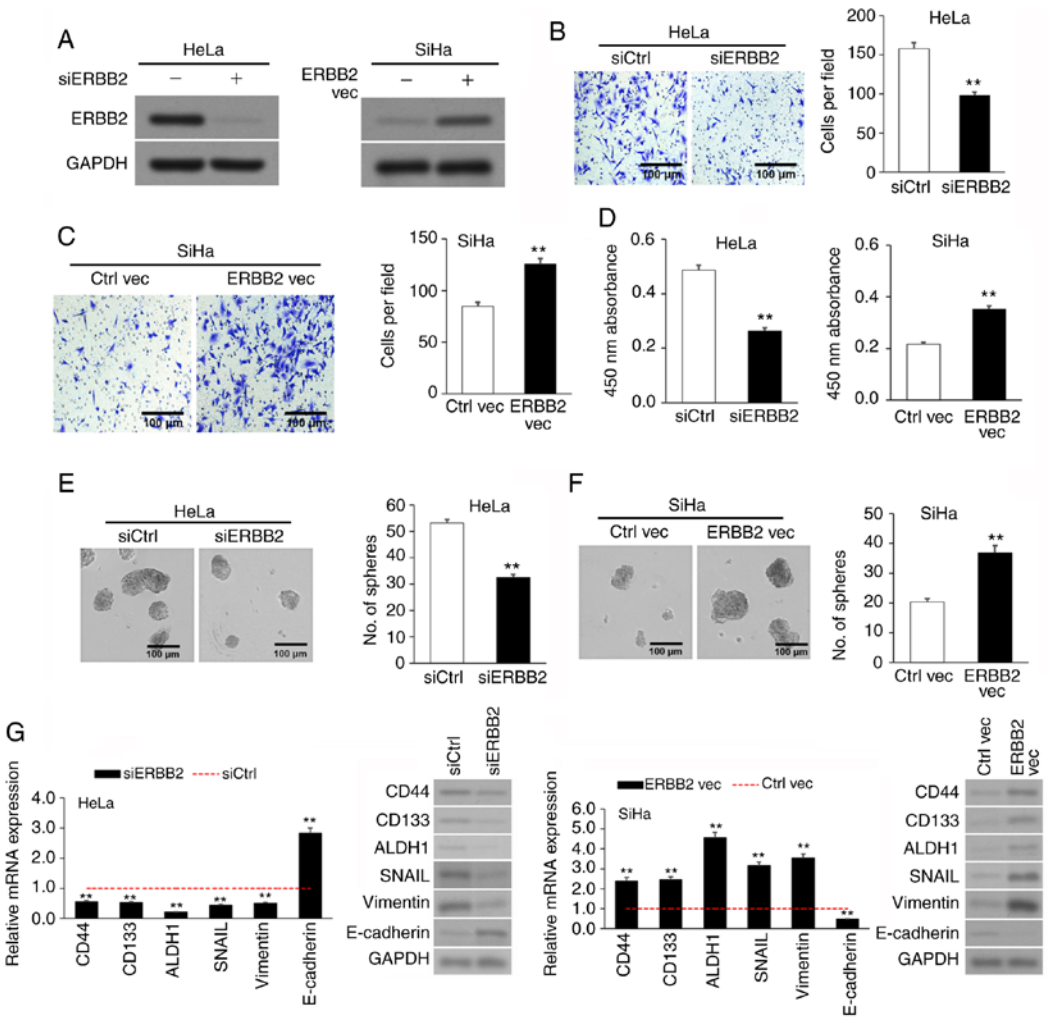

Figure 2. ERBB2 overexpression in cervical cancer cell lines stimulates viability, invasion and sphere-formation. (A) Confirmation of ERBB2 KD in siERBB2 cells and OE in ERBB2 vec cells via WB. GAPDH was used as the loading control. (B) Invasion of siERBB2 vs. siCtrl cells via Transwell assay. (C) Invasion of ERBB2 vec vs. Ctrl vec cells via Transwell assay. (D) Cellular viability of siERBB2, siCtrl, ERBB2 vec and Ctrl vec cells quantified using a Cell Counting Kit-8. (E) Sphere-formation of siERBB2 vs. siCtrl cells. (F) Sphere-formation of ERBB2 vec vs. Ctrl vec cells. (G) Analysis of metastasis-associated and cancer stem cell biomarkers mRNA and protein expression in siERBB2, siCtrl, ERBB2 vec and Ctrl vec cells via RT-qPCR and WB, respectively. GAPDH was used as the RT-qPCR housekeeping control and WB loading control. Data are expressed as the mean ± SEM (n=3). **P<0.01 vs. siCtrl or Ctrl vec analyzed via unpaired Student's t-test. KD, knockdown; OE, overexpression; WB, western blotting; RT-qPCR, reverse transcription-quantitative PCR; si, small interfering; Ctrl, control; vec, vector; ERBB2, Erb-B2 Receptor Tyrosine Kinase 2.

viability, invasion and sphere-formation. PIK3CA vec resulted in a partial rescuing of ERBB2-siRNA-mediated attenuation of cellular viability, invasion and sphere-formation (Fig. 3G-I). Overall, the present findings suggested that ERBB2 promoted an aggressive phenotype in cervical cancer cells via stimulating PIK3CA activity.

miR-3184-5p attenuates cervical cancer cell viability and invasion by targeting ERBB2. The TargetScan database was used to search for candidate miRNAs that may regulate ERBB2. miR-3184-5p was identified as a candidate miRNA, with a putative binding site on the ERBB2 3'-UTR (Fig. 4A). Therefore, miR-3184-5p was selected for further investigation. The results revealed that miR-3184-5p expression in HeLa and SiHa cell lines was significantly lower compared with in the non-cancerous H8 cell line (Fig. 4B). Direct binding between miR-3184-5p and the ERBB2-3'-UTR was measured using the luciferase reporter plasmids ERBB2-3'-UTR^{WT} or ERBB2-3'-UTR^{MU}, which possessed WT or MU miR-3184-5p binding locations, respectively. In these experiments, HeLa and SiHa cells underwent co-transfection with the aforementioned WT or MU reporter plasmids in addition to either miR-3184-5p mimics or inhibitors (Fig. S3). The luciferase signal emitted by the WT reporter plasmid was significantly lower when transfected with miR-3184-5p mimics and significantly higher when transfected with miR-3184-5p inhibitors (Fig. 4C and D). On the other hand, the signal emitted by the MU reporter plasmid was not affected by miR-3184-5p mimics or inhibitors (Fig. 4C and D). These findings suggested that miR-3184-5p may directly bind to ERBB2-3'-UTR^{WT} to regulate its expression. Additionally, ERBB2 and p-AKT protein expression was decreased in HeLa cells transfected with miR-3184-5p mimics (Fig. 4E), but was increased in SiHa cells transfected with miR-3184-5p inhibitors (Fig. 4F). Furthermore, ERBB2-OE in HeLa cultures rescued miR-3184-5p-induced attenuation of cellular viability, invasion and sphere-formation (Fig. 4G-I). These experiments demonstrated that miR-3184-5p directly interacted with the ERBB2 3'-UTR and inhibited ERBB2

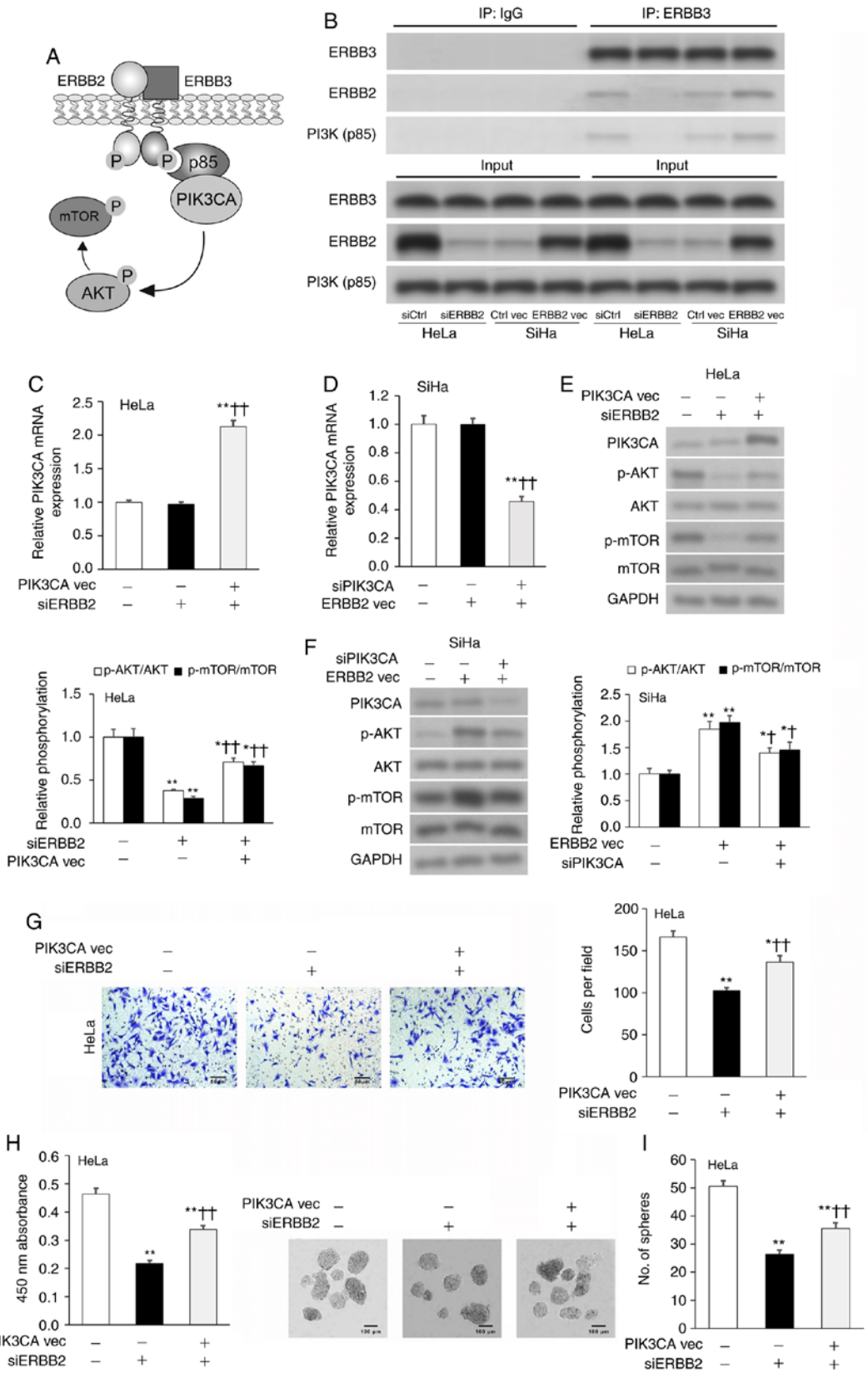

Figure 3. ERBB2 controls cervical cancer cell viability and invasion by regulating PIK3CA protein expression. (A) Schematic diagram of the ERBB2-ERRB3 complex interacting with PI3K(p85), thereby promoting the downstream phosphorylation of AKT and mTOR. (B) IP in cervical cancer cell lysates with antibodies against ERBB3 or IgG control. Expression levels of ERBB3, ERBB2 and PI3K(p85) in the IP fraction were assessed via WB. PIK3CA mRNA expression in transfected (C) HeLa and (D) SiHa cells assessed via RT-qPCR. GAPDH was used as the housekeeping control. PIK3CA, p-AKT/AKT and p-mTOR/mTOR protein expression in transfected (E) HeLa and (F) SiHa cells assessed via WB. GAPDH was used as the loading control. (G) Invasion of transfected HeLa cells assessed via Transwell assay. (H) Cellular viability of transfected HeLa cells quantified using Cell Counting Kit-8. (I) Sphere-formation of transfected HeLa cells. Data are expressed as the mean ± SEM (n=3). *P<0.05 and **P<0.01 vs. siCtrl or Ctrl vec; †P<0.05 and ††P<0.01 vs. siERBB2 or ERBB2 vec. Data were analyzed via one-way ANOVA. IP, immunoprecipitation; WB, western blotting; RT-qPCR, reverse transcription-quantitative PCR; si, small interfering; vec, vector; ERBB2, Erb-B2 Receptor Tyrosine Kinase 2; p-, phosphorylated; PIK3CA, phosphatidylinositol-4,5-bisphosphate 3-kinase catalytic subunit α.

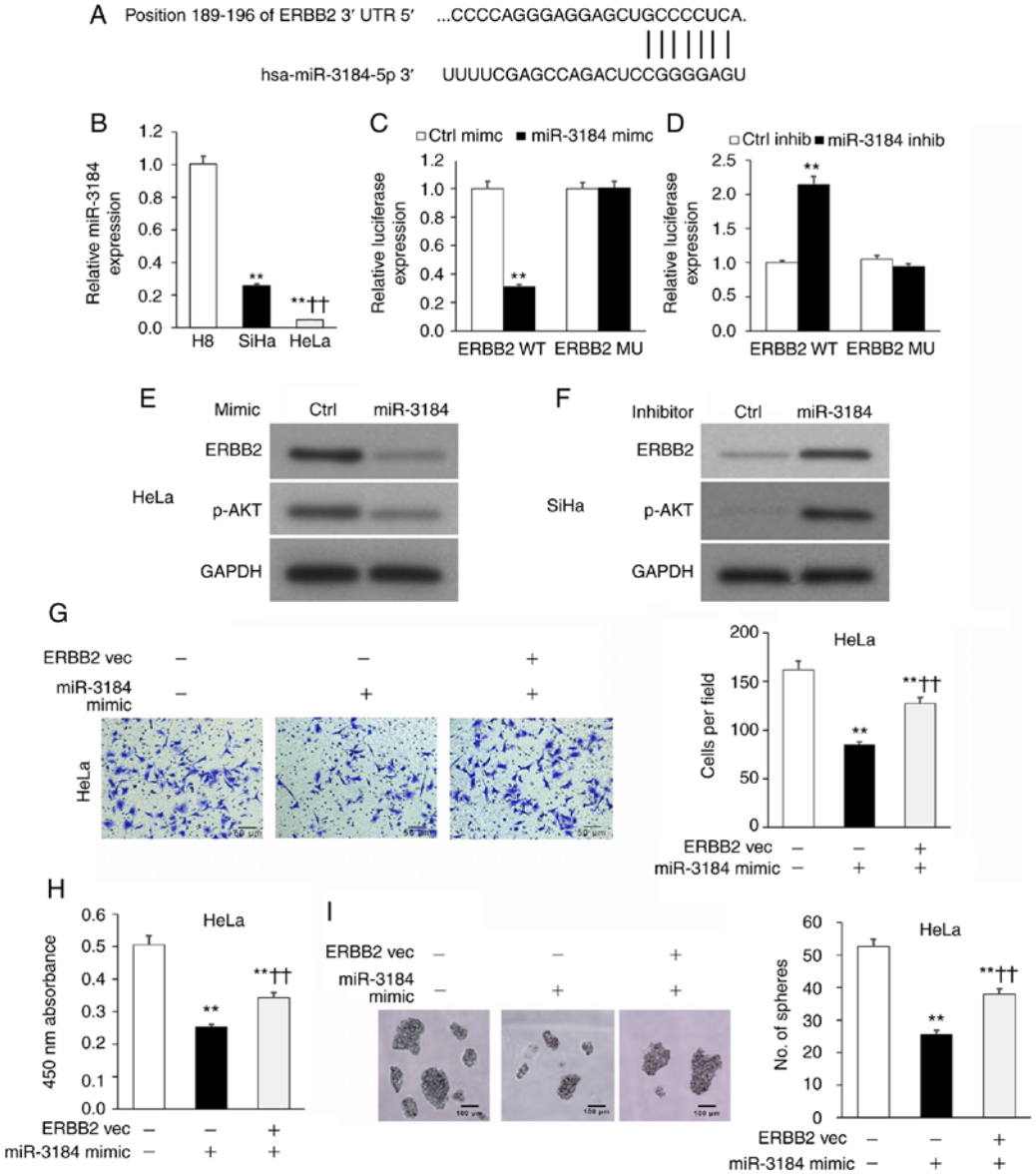

Figure 4. miR-3184-5p attenuates cervical cancer cell viability and invasion by targeting ERBB2. (A) Putative binding location for miR-3184-5p on ERBB2 3'-UTR via TargetScan analysis. (B) miR-3184-5p expression in HeLa and SiHa cervical cancer cell lines compared with in the non-cancerous human H8 cervical epithelial cell line assessed via RT-qPCR. U6 was used as the housekeeping control. **P<0.01 vs. H8; ††P<0.01 vs. SiHa. Luciferase reporter assay of ERBB2-3'-UTR^{WT} or ERBB2-3'-UTR^{MU} in (C) HeLa or (D) SiHa cells transfected with miR-3184-5p mimic or inhibitor, respectively. **P<0.01 vs. Ctrl mimic or Ctrl inhib. WB of (E) HeLa and (F) SiHa cells transfected with miR-3184-5p mimic or inhibitor, respectively. (G) Invasion of transfected HeLa cells assessed via Transwell assay. (H) Cellular viability of transfected HeLa cells quantified using Cell Counting Kit-8. (I) Sphere-formation of transfected HeLa cells. Data are expressed as the mean ± SEM (n=3). **P<0.01 vs. Ctrl vec; ††P<0.01 vs. miR-3184-5p mimic. Data were analyzed via one-way ANOVA. UTR, untranslated region; WT, wild-type; MU, mutant; Ctrl, control; inhib, inhibitor; WB, western blotting; RT-qPCR, reverse transcription-quantitative PCR; miR, microRNA; vec, vector; ERBB2, Erb-B2 Receptor Tyrosine Kinase 2; PIK3CA, phosphatidylinositol-4,5-bisphosphate 3-kinase catalytic subunit α.

expression, thereby promoting a less aggressive cervical cancer phenotype.

miR-3184-5p expression is lower in patient-derived cervical cancer biopsy tissues and low miR-3184-5p expression is associated with a poor prognosis. The association of miR-3184-5p with clinicopathological cervical cancer characteristics was assessed in patient-derived biopsies. miR-3184-5p expression was significantly lower in cervical cancer biopsy specimens compared with in neighboring matched healthy tissues (Fig. S4A) and significantly lower in patients with late-stage (Fig. S4B) and lymph node metastatic disease (Fig. S4C) compared with in patients with early stage and no lymph node metastasis. Kaplan-Meier analysis revealed that low miR-3184-5p expression was associated with poorer patient survival outcomes compared with high miR-3184-5p expression (Fig. S4D). Overall, the data demonstrated that miR-3184-5p expression was negatively associated with clinicopathological indicators of cervical cancer progression.

Mithramycin A-induced p53 activation boosts miR-3184-5p expression, which lowers ERBB2 expression and attenuates the viability and invasion of cervical cancer cell lines. Since the tumor suppressor p53 stimulates miR-3184 expression (43), it was hypothesized that incubation of cervical cancer cells with the p53 activator Mithramycin A (44) would enhance miR-3184-5p

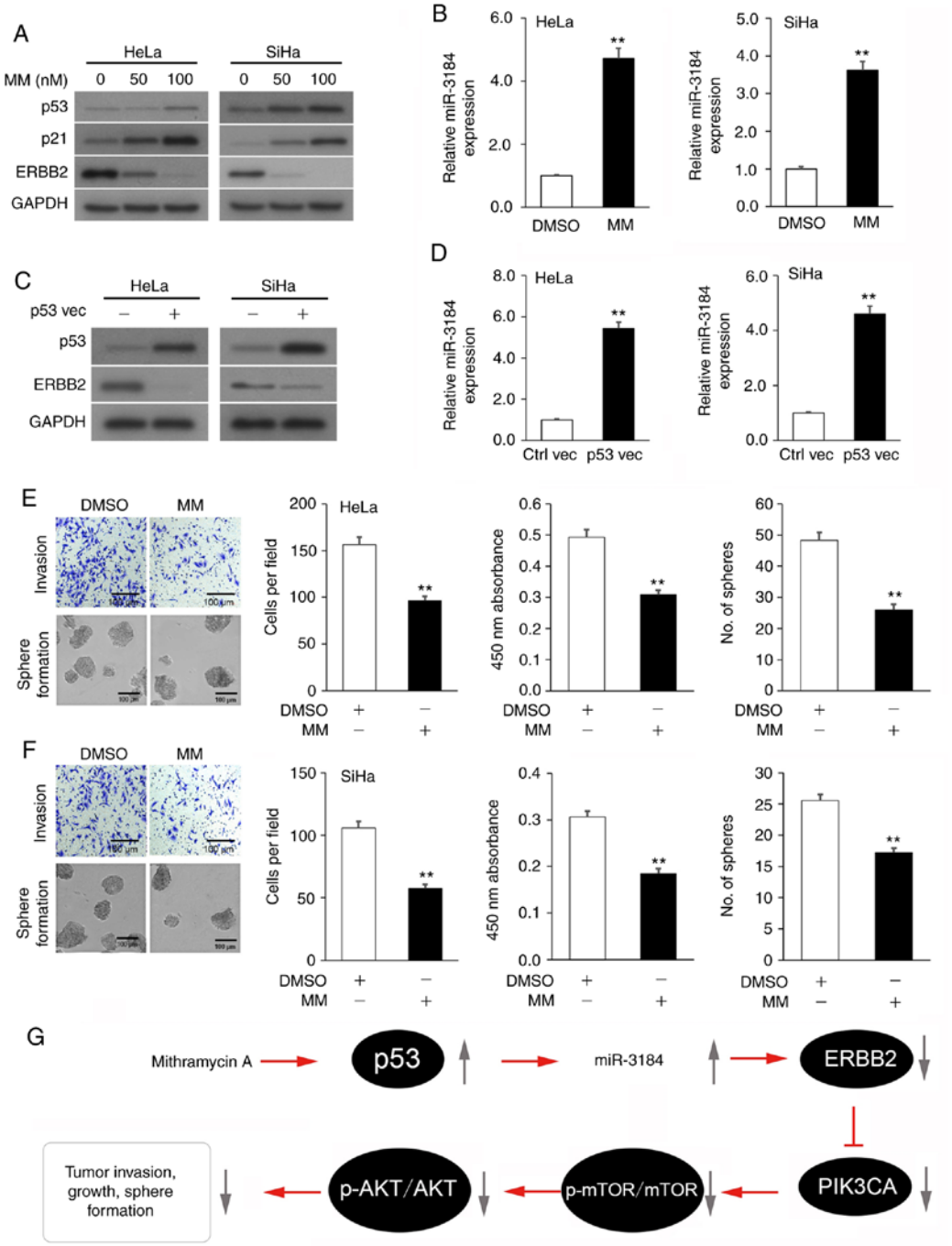

Figure 5. p53-activating Mithramycin A boosts miR-3184-5p expression, which lowers ERBB2 expression and attenuates viability and invasion of cervical cancer cell lines. (A) p53, p21 and ERBB2 protein expression in cervical cancer cultures incubated with MM or vehicle (DMSO) assessed via WB. GAPDH was used as the loading control. (B) miR-3184-5p expression in cervical cancer cultures incubated with MM or vehicle assessed via RT-qPCR. U6 was used as the housekeeping control. (C) p53 and ERBB2 protein expression in cervical cancer cultures transfected with a p53 overexpression plasmid or empty plasmid control assessed via WB. GAPDH was used as the loading control. (D) miR-3184-5p expression in cervical cancer cultures transfected with a p53 overexpression plasmid or empty plasmid control assessed via RT-qPCR. U6 was used as the housekeeping control. (E) Representative images of Transwell and sphere-formation assays in (E) HeLa and (F) SiHa cells, and quantitative analysis of viability, invasion and sphere-formation of cells treated with MM or vehicle. (G) Schematic diagram of the p53 activator MM rescuing miR-3184-5p expression, thereby suppressing ERBB2 transcription. This attenuates PIK3CA activity, which stimulates cervical cancer cell viability, invasion and sphere-formation. Data are expressed as the mean ± SEM (n=3). **P<0.01 analyzed via unpaired Student's t-test. MM, Mithramycin A; Ctrl, control; WB, western blotting; RT-qPCR, reverse transcription-quantitative PCR; miR, microRNA; vec, vector; ERBB2, Erb-B2 Receptor Tyrosine Kinase 2; p-, phosphorylated; PIK3CA, phosphatidylinositol-4,5-bisphosphate 3-kinase catalytic subunit α.

expression and would consequently suppress ERBB2 expression, cellular viability and invasion. Indeed, incubation of HeLa and SiHa cultures with Mithramycin A increased the expression levels of p53 and its downstream mediator p21 in a dose-dependent manner, while decreasing ERBB2 expression, compared with the vehicle control cultures (Fig. 5A). As predicted, HeLa and SiHa cells expressed a concurrent increase in miR-3184-5p (Fig. 5B). Subsequently, HeLa and SiHa cultures underwent transfection with a TP53 OE plasmid to test whether p53 controlled miR-3184-5p and ERBB2 expression. As expected, TP53 OE in

HeLa and SiHa cultures decreased ERBB2 expression (Fig. 5C) and increased miR-3184-5p expression (Fig. 5D). Lastly, incubation of HeLa and SiHa cultures with Mithramycin A significantly decreased cell viability, invasion and sphere-formation compared with vehicle control cultures (Fig. 5E and F). Overall, these experiments indicated that Mithramycin A-induced p53 activation promoted miR-3184-5p expression, which in turn inhibited ERBB2 expression, as well as viability and invasion of cervical cancer cells (Fig. 5G).

Discussion

Cervical cancer continues to be among the more prevalent types of cancer in women globally and was responsible for over a quarter million mortalities in 2012 (2). To develop improved cervical cancer treatment options, a deeper knowledge of its molecular determinants is required. The *ERBB2* gene is frequently mutated in several solid tumors, with the following types of tumor exhibiting the highest incidence of *ERBB2* mutations: Bladder cancer (16.6%), small intestine cancer (8.6%), ampullar cancer (6.5%), non-melanoma skin cancer (6.1%) and cervical cancer (5.5%) (45). ERBB2 upregulation has been associated with higher tumor grades and more advanced staging in patients with bladder cancer (46). On a cellular level, ERBB2 is known to increase the aggressiveness of breast tumor cells and help them acquire resistance to conventional chemotherapies (47-49). Molecularly, ERBB2 is known to heterodimerize with other HER/EGFR family members to affect downstream cascades associated with anti-apoptotic mechanisms, cell proliferation and cell invasiveness (50). For example, ERBB2 stimulates the downstream oncogenic, multidrug-resistance-conferring PI3K/AKT axis in breast adenocarcinoma cells through its heterodimerization with ERBB3 (38,39,51).

In contrast to other solid tumors, the relevance of ERBB2 expression in cervical cancer has not been fully investigated. Therefore, the present study examined the role of ERBB2 in cervical cancer. First, ERBB2 expression was analyzed in patient-derived cervical cancer and matched healthy cervical tissues, which revealed that elevated ERBB2 expression in tumors was associated with poorer patient survival outcomes compared with low ERBB2 expression. In HeLa and SiHa cell lines, OE of ERBB2 increased cell viability, invasion and sphere-formation, while KD of ERBB2 produced the opposite effect. The present results revealed that OE of ERBB2 drove activation of PIK3CA and downstream AKT phosphorylation, which are both crucial oncoproteins, via promoting ERBB3-PI3K(p85) binding. Notably, *ERBB2* mutations frequently co-occur with *PIK3CA* mutations in malignant tumors (21.4%) (45). The current data highlighted the relevance of upregulated ERBB2 expression in cervical cancer, which may foster an aggressive cervical cancer phenotype by driving PIK3CA/p-AKT axis activity.

ERBB2 expression in cancer cells is regulated via numerous cellular pathways, such as the estrogen receptor-PAX2 pathway, the MKK6/p38 MAPK pathway and the Neu differentiation factor pathway (52-54). miRNA-mediated regulation of ERBB2 expression is of increasing interest to cancer research; for instance, it has been demonstrated that miR-34a and miR-155 can suppress ERBB2-induced pro-malignant effects in breast cancer cells (55,56). The possibility of miRNA-dependent aberrant ERBB2 expression in cervical cancer has not been investigated. The present study revealed that miR-3184-5p expression was lower in cervical cancer biopsies compared with in matched control cervical tissues. Furthermore, a direct interaction between miR-3184-5p and ERBB2 3'-UTR was demonstrated, suggesting that miR-3184-5p may block ERBB2 to promote a less aggressive cervical cancer phenotype. The current study revealed a miR-3184-5p-dependent pathway for the negative regulation of ERBB2 in cervical cancer. This novel discovery suggested that normalization of miR-3184-5p expression may ameliorate the cervical cancer phenotype and that this miRNA may be used as a possible therapeutic avenue.

Mithramycin A attenuates the proliferation of diverse types of cancer, such as cervical cancer, via lowering the levels of the transcription factor SP1 (23,57,58), and stimulates p53 activation *in vitro* and *in vivo* (24). Since the tumor suppressor p53 induces miR-3184-5p expression (43), the present study hypothesized that Mithramycin A may restore miR-3184-5p expression in a p53-dependent manner. Indeed, treatment of HeLa and SiHa cultures with Mithramycin A increased p53 and miR-3184-5p expression, while lowering ERBB2 expression, which led to decreased cell viability, invasion and sphere-formation. Notably, *ERBB2* mutations frequently co-occur with *TP53* mutations in malignant tumors (59.5%) (45). Mithramycin A possesses a favorable safety profile following long-term treatment in mouse cervical cancer xenograft models (23), advocating Mithramycin A as a potential cervical cancer treatment option.

There are a few limitations to the present study. First, the study was limited to an *in vitro* investigation of the p53/miR-3184-5p/ERBB2 axis in patient-derived cervical cancer samples and established cell lines. Future work should examine the role of this axis in animal models of cervical cancer. Second, p53, as a key tumor suppressor, has a multitude of downstream targets that regulate cell proliferation, migration, metastasis and cell cycle progression (59); however, it is infeasible to study all p53 downstream signaling pathways in a single study. Therefore, the scope of the current study was solely focused on identifying and establishing the effects of the p53/miR-3184-5p/ERBB2 axis in cervical cancer cells.

In conclusion, the present study reported the involvement of the p53/miR-3184-5p/ERBB2 axis in promoting cervical cancer development via PIK3CA. Treatment of cervical cancer cells with the p53 activator Mithramycin A restored the levels of the endogenous ERBB2 inhibitor miR-3184-5p and may constitute a novel treatment strategy for cervical cancer.

Acknowledgements

Not applicable.

Funding

The present study was supported by the Natural Science Foundation of Bengbu Medical College (grant no. BYKF1726), the Anhui Provincial Natural Science Foundation (grant no. 1908085MH252) and the Key Program of Natural Science Research of Higher Education of Anhui Province (grant no. KJ2019A0346).

Availability of data and materials

The datasets used and/or analyzed during the current study are available from the corresponding author on reasonable request.

Authors' contributions

HL conceived and designed the study. YL, JZ, NW, FL and LW performed the experiments. YZ, JL, XZ, SG and HW analyzed the data. HL drafted the manuscript. All authors read and approved the final version of the manuscript.

Ethics approval and consent to participate

The present study was approved by the Ethics Review Committee of the First Affiliated Hospital of Bengbu Medical College (approval no. 201858; Bengbu, China). Patients who donated cervical cancer tissues gave their informed consent in writing prior to their involvement in the study.

Patient consent for publication

Not applicable.

Competing interests

The authors declare that they have no competing interests.

References

1. Siegel RL, Miller KD and Jemal A: Cancer statistics, 2016. CA A Cancer J Clin 66: 7-30, 2016.
2. Torre LA, Bray F, Siegel RL, Ferlay J, Lortet-Tieulent J and Jemal A: Global cancer statistics, 2012. CA A Cancer J Clin 65: 87-108, 2015.
3. Colombo N, Carinelli S, Colombo A, Marini C, Rollo D and Sessa C; ESMO Guidelines Working Group: Cervical cancer: ESMO Clinical Practice Guidelines for diagnosis, treatment and follow-up. Ann Oncol 23 (Suppl 7): vii27-vii32, 2012.
4. Manzo-Merino J, Contreras-Paredes A, Vázquez-Ulloa E, Rocha-Zavaleta L, Fuentes-Gonzalez AM and Lizano M: The role of signaling pathways in cervical cancer and molecular therapeutic targets. Arch Med Res 45: 525-539, 2014.
5. Konno Y, Dong P, Xiong Y, Suzuki F, Lu J, Cai M, Watari H, Mitamura T, Hosaka M, Hanley SJ, *et al*: MicroRNA-101 targets EZH2, MCL-1 and FOS to suppress proliferation, invasion and stem cell-like phenotype of aggressive endometrial cancer cells. Oncotarget 5: 6049-6062, 2014.
6. Liang X, Liu Y, Zeng L, Yu C, Hu Z, Zhou Q and Yang Z: miR-101 inhibits the G1-to-S phase transition of cervical cancer cells by targeting Fos. Int J Gynecol Cancer 24: 1165-1172, 2014.
7. Cheung T, Leung J, Chung TK, Lam S, To K and Wong Y: C-fos overexpression is associated with the pathoneogenesis of invasive cervical cancer. Gynecol Obstet Invest 43: 200-203, 1997.
8. Dong P, Ihira K, Hamada J, Watari H, Yamada T, Hosaka M, Hanley SJ, Kudo M and Sakuragi N: Reactivating p53 functions by suppressing its novel inhibitor iASPP: A potential therapeutic opportunity in p53 wild-type tumors. Oncotarget 6: 19968-19975, 2015.
9. Dong P, Xiong Y, Watari H, Hanley SJ, Konno Y, Ihira K, Suzuki F, Yamada T, Kudo M, Yue J and Sakuragi N: Suppression of iASPP-dependent aggressiveness in cervical cancer through reversal of methylation silencing of microRNA-124. Sci Rep 6: 35480, 2016.
10. Xiong Y, Sun F, Dong P, Watari H, Yue J, Yu MF, Lan CY, Wang Y and Ma ZB: iASPP induces EMT and cisplatin resistance in human cervical cancer through miR-20a-FBXL5/BTG3 signaling. J Exp Clin Cancer Res 36: 48, 2017.
11. Romaine SP, Tomaszewski M, Condorelli G and Samani NJ: MicroRNAs in cardiovascular disease: An introduction for clinicians. Heart 101: 921-928, 2015.
12. Sun NX, Ye C, Zhao Q, Zhang Q, Xu C, Wang SB, Jin ZJ, Sun SH, Wang F and Li W: Long noncoding RNA-EBIC promotes tumor cell invasion by binding to EZH2 and repressing E-cadherin in cervical cancer. PLoS One 9: e100340, 2014.
13. Hu X, Schwarz JK, Lewis JS Jr, Huettner PC, Rader JS, Deasy JO, Grigsby PW and Wang X: A microRNA expression signature for cervical cancer prognosis. Cancer Res 70: 1441-1448, 2010.
14. Hattori H, Janky RS, Nietfeld W, Aerts S, Madan Babu M and Venkitaraman AR: p53 shapes genome-wide and cell type-specific changes in microRNA expression during the human DNA damage response. Cell Cycle 13: 2572-2586, 2014.
15. Croessmann S, Formisano L, Kinch LN, Gonzalez-Ericsson PI, Sudhan DR, Nagy RJ, Mathew A, Bernicker EH, Cristofanilli M, He J, *et al*: Combined blockade of activating ERBB2 mutations and ER results in synthetic lethality of ER+/HER2 mutant breast cancer. Clin Cancer Res 25: 277-289, 2019.
16. Sanchez-Vega F, Hechtman JF, Castel P, Castel P, Ku GY, Tuvy Y, Won H, Fong CJ, Bouvier N, Nanjangud GJ, *et al*: EGFR and MET amplifications determine response to HER2 inhibition in ERBB2-amplified esophagogastric cancer. Cancer Discov 9: 199-209, 2019.
17. Ross JS, Fakih M, Ali SM, Elvin JA, Schrock AB, Suh J, Vergilio JA, Ramkissoon S, Severson E, Daniel S, *et al*: Targeting HER2 in colorectal cancer: The landscape of amplification and short variant mutations in ERBB2 and ERBB3. Cancer 124: 1358-1373, 2018.
18. Xiang L, Jiang W, Ye S, He T, Pei X, Li J, Chan DW, Ngan HYS, Li F, Tao P, *et al*: ERBB2 mutation: A promising target in non-squamous cervical cancer. Gynecol Oncol 148: 311-316, 2018.
19. Barceló F, Ortiz-Lombardia M, Martorell M, Oliver M, Méndez C, Salas JA and Portugal J: DNA binding characteristics of mithramycin and chromomycin analogues obtained by combinatorial biosynthesis. Biochemistry 49: 10543-10552, 2010.
20. Kennedy B and Torkelson JL: Long-term follow-up of stage III testicular carcinoma treated with mithramycin (Plicamycin). Med Pediatr Oncol 24: 327-328, 1995.
21. Dutcher JP, Coletti D, Paietta E and Wiernik PH: A pilot study of alpha-interferon and plicamycin for accelerated phase of chronic myeloid leukemia. Leuk Res 21: 375-380, 1997.
22. Fernández-Guizán A, Mansilla S, Barceló F, Barceló F, Vizcaíno C, Núñez LE, Morís F, González S and Portugal J: The activity of a novel mithramycin analog is related to its binding to DNA, cellular accumulation, and inhibition of Sp1-driven gene transcription. Chem Biol Interact 219: 123-132, 2014.
23. Choi ES, Nam JS, Jung JY, Cho NP and Cho SD: Modulation of specificity protein 1 by mithramycin A as a novel therapeutic strategy for cervical cancer. Sci Rep 4: 7162, 2014.
24. Rao M, Atay SM, Shukla V, Hong Y, Upham T, Ripley RT, Hong JA, Zhang M, Reardon E, Fetsch P, *et al*: Mithramycin depletes specificity protein 1 and activates p53 to mediate senescence and apoptosis of malignant pleural mesothelioma cells. Clin Cancer Res 22: 1197-1210, 2016.
25. Thorpe LM, Yuzugullu H and Zhao JJ: PI3K in cancer: Divergent roles of isoforms, modes of activation and therapeutic targeting. Nat Rev Cancer 15: 7, 2015.
26. Wright AA, Howitt BE, Myers AP, Dahlberg SE, Palescandolo E, Van Hummelen P, MacConaill LE, Shoni M, Wagle N, Jones RT, *et al*: Oncogenic mutations in cervical cancer: Genomic differences between adenocarcinomas and squamous cell carcinomas of the cervix. Cancer 119: 3776-3783, 2013.
27. Benedet J, Pecorelli S, Ngan H and Hacker NF: Staging classifications and clinical practice guidelines for gynaecological cancers. Int J Gynecol Obstetr 70: 207-312, 2000.
28. Gioia G, Werner B, Nydam D and Moroni P: Validation of a mycoplasma molecular diagnostic test and distribution of mycoplasma species in bovine milk among New York State dairy farms. J Dairy Sci 99: 4668-4677, 2016.
29. Livak KJ and Schmittgen TD: Analysis of relative gene expression data using real-time quantitative PCR and the 2(-Delta Delta C(T)) method. Methods 25: 402-408, 2001.
30. Dong P, Xiong Y, Watari H, Hanley SJ, Konno Y, Ihira K, Yamada T, Kudo M, Yue J and Sakuragi N: MiR-137 and miR-34a directly target Snail and inhibit EMT, invasion and sphere-forming ability of ovarian cancer cells. J Exp Clin Cancer Res 35: 132, 2016.
31. Ihira K, Dong P, Xiong Y, Watari H, Konno Y, Hanley SJ, Noguchi M, Hirata N, Suizu F, Yamada T, *et al*: EZH2 inhibition suppresses endometrial cancer progression via miR-361/Twist axis. Oncotarget 8: 13509-13520, 2017.

32. Hsiao YH, Hsieh MJ, Yang SF, Chen SP, Tsai WC and Chen PN: Phloretin suppresses metastasis by targeting protease and inhibits cancer stemness and angiogenesis in human cervical cancer cells. Phytomedicine 62: 152964, 2019.
33. Hu Y, Ma Y, Liu J, Cai Y, Zhang M and Fang X: LINC01128 expedites cervical cancer progression by regulating miR-383-5p/SFN axis. BMC Cancer 19: 1-11, 2019.
34. Lv Y, Cang W, Li Q, Liao X, Zhan M, Deng H, Li S, Jin W, Pang Z, Qiu X, *et al*: Erlotinib overcomes paclitaxel-resistant cancer stem cells by blocking the EGFR-CREB/GRβ-IL-6 axis in MUC1-positive cervical cancer. Oncogenesis 8: 70, 2019.
35. Han SA, Jang JH, Won KY, Lim SJ and Song JY: Prognostic value of putative cancer stem cell markers (CD24, CD44, CD133, and ALDH1) in human papillary thyroid carcinoma. Pathol Res Pract 213: 956-963, 2017.
36. Mizukami T, Kamachi H, Mitsuhashi T, Tsuruga Y, Hatanaka Y, Kamiyama T, Matsuno Y and Taketomi A: Immunohistochemical analysis of cancer stem cell markers in pancreatic adenocarcinoma patients after neoadjuvant chemoradiotherapy. BMC Cancer 14: 687, 2014.
37. Engelman JA: Targeting PI3K signalling in cancer: Opportunities, challenges and limitations. Nat Rev Cancer 9: 550-562, 2009.
38. Siegel PM, Ryan ED, Cardiff RD and Muller WJ: Elevated expression of activated forms of Neu/ErbB-2 and ErbB-3 are involved in the induction of mammary tumors in transgenic mice: Implications for human breast cancer. EMBO J 18: 2149-2164, 1999.
39. Zhou BP, Hu MC, Miller SA, Yu Z, Xia W, Lin SY and Hung MC: HER-2/neu blocks tumor necrosis factor-induced apoptosis via the Akt/NF-kappaB pathway. J Biol Chem 275: 8027-8031, 2000.
40. Prigent SA and Gullick WJ: Identification of c-erbB-3 binding sites for phosphatidylinositol 3'-kinase and SHC using an EGF receptor/c-erbB-3 chimera. EMBO J 13: 2831-2841, 1994.
41. Vasudevan KM, Barbie DA, Davies MA, Rabinovsky R, McNear CJ, Kim JJ, Hennessy BT, Tseng H, Pochanard P, Kim SY, *et al*: AKT-independent signaling downstream of oncogenic PIK3CA mutations in human cancer. Cancer Cell 16: 21-32, 2009.
42. Bonazzoli E, Cocco E, Lopez S, Bellone S, Zammataro L, Bianchi A, Manzano A, Yadav G, Manara P, Perrone E, *et al*: PI3K oncogenic mutations mediate resistance to afatinib in HER2/neu overexpressing gynecological cancers. Gynecol Oncol 153: 158-164, 2019.
43. Suzuki HI, Yamagata K, Sugimoto K, Iwamoto T, Kato S and Miyazono K: Modulation of microRNA processing by p53. Nature 460: 529-533, 2009.
44. Dong P, Xiong Y, Hanley SJ, Yue J and Watari H: Musashi-2, a novel oncoprotein promoting cervical cancer cell growth and invasion, is negatively regulated by p53-induced miR-143 and miR-107 activation. J Exp Clin Cancer Res 36: 150, 2017.
45. Cousin S, Khalifa E, Crombe A, Laizet Y, Lucchesi C, Toulmonde M, Le Moulec S, Auzanneau C, Soubeyran I and Italiano A: Targeting ERBB2 mutations in solid tumors: Biological and clinical implications. J Hematol Oncol 11: 86, 2018.
46. Breyer J, Wirtz RM, Laible M, Schlombs K, Erben P, Kriegmair MC, Stoehr R, Eidt S, Denzinger S, Burger M, *et al*: ESR1, ERBB2, and Ki67 mRNA expression predicts stage and grade of non-muscle-invasive bladder carcinoma (NMIBC). Virchows Arch 469: 547-552, 2016.
47. Ursini-Siegel J, Schade B, Cardiff RD and Muller WJ: Insights from transgenic mouse models of ERBB2-induced breast cancer. Nat Rev Cancer 7: 389-397, 2007.
48. Di Cosimo S and Baselga J: Targeted therapies in breast cancer: Where are we now? Eur J Cancer 44: 2781-2790, 2008.
49. Hynes NE and Lane HA: ERBB receptors and cancer: The complexity of targeted inhibitors. Nat Rev Cancer 5: 341-354, 2005.
50. Olayioye MA, Neve RM, Lane HA and Hynes NE: The ErbB signaling network: Receptor heterodimerization in development and cancer. EMBO J 19: 3159-3167, 2000.
51. Knuefermann C, Lu Y, Liu B, Jin W, Liang K, Wu L, Schmidt M, Mills GB, Mendelsohn J and Fan Z: HER2/PI-3K/Akt activation leads to a multidrug resistance in human breast adenocarcinoma cells. Oncogene 22: 3205-3212, 2003.
52. Hurtado A, Holmes KA, Geistlinger TR, Hutcheson IR, Nicholson RI, Brown M, Jiang J, Howat WJ, Ali S and Carroll JS: Regulation of ERBB2 by oestrogen receptor-PAX2 determines response to tamoxifen. Nature 456: 663-666, 2008.
53. Demidov ON, Kek C, Shreeram S, Timofeev O, Fornace AJ, Appella E and Bulavin DV: The role of the MKK6/p38 MAPK pathway in Wip1-dependent regulation of ErbB2-driven mammary gland tumorigenesis. Oncogene 26: 2502-2506, 2007.
54. Daly JM, Jannot CB, Beerli RR, Graus-Porta D, Maurer FG and Hynes NE: Neu differentiation factor induces ErbB2 down-regulation and apoptosis of ErbB2-overexpressing breast tumor cells. Cancer Res 57: 3804-3811, 1997.
55. Wang Y, Zhang X, Chao Z, Kung HF, Lin MC, Dress A, Wardle F, Jiang BH and Lai L: MiR-34a modulates ErbB2 in breast cancer. Cell Biol Int 41: 93-101, 2017.
56. He XH, Zhu W, Yuan P, Jiang S, Li D, Zhang HW and Liu MF: miR-155 downregulates ErbB2 and suppresses ErbB2-induced malignant transformation of breast epithelial cells. Oncogene 35: 6015-6025, 2016.
57. Malek A, Núñez LE, Magistri M, Brambilla L, Jovic S, Carbone GM, Morís F and Catapano CV: Modulation of the activity of Sp transcription factors by mithramycin analogues as a new strategy for treatment of metastatic prostate cancer. PLoS One 7: e35130, 2012.
58. Wang L, Guan X, Zhang J, Jia Z, Wei D, Li Q, Yao J and Xie K: Targeted inhibition of Sp1-mediated transcription for antiangiogenic therapy of metastatic human gastric cancer in orthotopic nude mouse models. Int J Oncol 33: 161-167, 2008.
59. Haupt S, Raghu D and Haupt Y: Mutant p53 drives cancer by subverting multiple tumor suppression pathways. Front Oncol 6: 12, 2016.